A novel endothelial-specific heat shock protein HspA12B is required in both zebrafish development and endothelial functions in vitro

Guang Hu[1,*], Jian Tang[1,*], Bo Zhang[1,*], Yanfeng Lin[1,*], Jun-ichi Hanai[1,*], Jenna Galloway[2], Victoria Bedell[3], Nathan Bahary[4], Zhihua Han[5], Ramani Ramchandran[3], Bernard Thisse[6], Christine Thisse[6], Leonard I. Zon[2] and Vikas P. Sukhatme[1,‡]

[1]Renal Division, Center for Study of the Tumor Microenvironment and Center for Vascular Biology Research, Department of Medicine, Beth Israel Deaconess Medical Center, Boston, MA 02215, USA
[2]Division of Hematology/Oncology, Children's Hospital, Department of Medicine, Boston, MA 02215, USA
[3]National Cancer Institute, National Institutes of Health, Rockville, MD 20850, USA
[4]Molecular Genetics and Biochemistry, University of Pittsburgh School of Medicine, W1257 BSTWR, Pittsburgh, PA 15261, USA
[5]Department of Biochemistry and Molecular Biology, East Tennessee State University, Johnson City, TN 37614, USA
[6]Institut de Biologie Moleculaire et Cellulaire, CNRS, INSERM, Universite Louis Pasteur, C. U. de Strasbourg, France

*These authors contributed equally to this work
‡Author for correspondence (e-mail: vsukhatm@bidmc.harvard.edu)

Accepted 20 July 2006
Journal of Cell Science 119, 4117-4126 Published by The Company of Biologists 2006
doi:10.1242/jcs.03179

Summary

A zebrafish transcript dubbed GA2692 was initially identified via a whole-mount in situ hybridization screen for vessel specific transcripts. Its mRNA expression during embryonic development was detected in ventral hematopoietic and vasculogenic mesoderm and later throughout the vasculature up to 48 hours post fertilization. Morpholino-mediated knockdown of GA2692 in embryos resulted in multiple defects in vasculature, particularly, at sites undergoing active capillary sprouting: the intersegmental vessels, sub-intestinal vessels and the capillary sprouts of the pectoral fin vessel. During the course of these studies, a homology search indicated that GA2692 is the zebrafish orthologue of mammalian HspA12B, a distant member of the heat shock protein 70 (Hsp70) family. By a combination of northern blot and real-time PCR analysis, we showed that HspA12B is highly expressed in human endothelial cells in vitro. Knockdown of HspA12B by small interfering RNAs (siRNAs) in human umbilical vein endothelial cells blocked wound healing, migration and tube formation, whereas overexpression of HspA12B enhanced migration and accelerated wound healing – data that are consistent with the in vivo fish phenotype obtained in the morpholino-knockdown studies. Phosphorylation of Akt was consistently reduced by siRNAs against HspA12B. Overexpression of a constitutively active form of Akt rescued the inhibitory effects of knockdown of HspA12B on migration of human umbilical vein endothelial cells. Collectively, our data suggests that HspA12B is a highly endothelial-cell-specific distant member of the Hsp70 family and plays a significant role in endothelial cells during development and angiogenesis in vitro, partially attributable to modulation of Akt phosphorylation.

Supplementary material available online at
http://jcs.biologists.org/cgi/content/full/119/19/4117/DC1

Key words: HspA12B, Zebrafish, Vascular development, Endothelial cells, Angiogenesis, Akt

Introduction

Recent studies have demonstrated the use of zebrafish to study vascular development (Chan et al., 2005; Kidd and Weinstein, 2003; Sumanas et al., 2005; Zhu et al., 2005). We have sought to discover new genes of functional importance in early vessel formation by a two-step process: (A) the screening of 4000 transcripts from a zebrafish kidney marrow cDNA library (Galloway et al., 2005) to identify those whose expression was relatively restricted to developing vessels in the 24-72 hours post fertilization (hpf) period and, (B) the use of antisense morpholino-oligonucleotide-mediated knockdown in embryos to assess a vascular phenotype. Of the approximately 50 transcripts from the library whose expressions were localized mainly to vasculature during early development, we focused attention on one, designated as GA2692. This transcript, at the time these studies were initiated, had homology to the human cDNA FLJ32150, and nothing was known in terms of its expression or function. More recently, FLJ32150 was found to be identical to HspA12B, a transcript present in macrophages in atherosclerotic lesions (Han et al., 2003), and a distantly related member of the Hsp70 family but one containing an atypical ATPase domain and a distinctive substrate binding domain located in its C-terminus.

Hsp70s constitute one group of the heat shock protein superfamily, classified according to their molecular mass: Hsp10, small Hsps, Hsp40, Hsp60, Hsp70, Hsp90 and Hsp110 (Kiang and Tsokos, 1998; Snoeckx et al., 2001). As molecular chaperones, mammalian Hsp70s associate with unfolded nascent precursor peptides to stabilize them prior to their folding into mature proteins and reaching their ultimate cellular

compartments (Artigues et al., 1997; Beckmann et al., 1990; Hartl et al., 1992). Hsp70s can also aid in solubilizing and refolding damaged proteins or transporting them to degradative organelles. Hsp70s are capable of protecting cells, tissues, organs and animals from various noxious conditions (Kiang et al., 1998; Marber et al., 1995; Plumier et al., 1995; Polla et al., 1987; Ribeiro et al., 1994; Samali and Cotter, 1996; Takano et al., 1998).

Here, we characterize the zebrafish GA2692 transcript and its presumed mammalian orthologue HspA12B and show their selective expression in vasculature in zebrafish and in endothelial cells (ECs) in vitro. Then, by using antisense morpholino oligonucleotides and small interfering RNA (siRNA), we demonstrate that GA2692/HspA12B (which for simplicity will henceforth be designated just as HspA12B) is essential for zebrafish vascular development and for endothelial cell migration, wound healing and tube formation in vitro.

Results

Zebrafish GA2692 cDNA sequence and homology to mammalian HspA12B

A clone designated GA2692 was one of the roughly 50 clones – from a total of approximately 4000 cDNAs screened by whole-mount in situ hybridization in zebrafish – that showed expression largely restricted to developing vessels.

The sequence of the GA2692 cDNA consisted of 2884 nucleotides (GenBank accession number, DQ119052). The longest open reading frame extended from nucleotides 267 to 2339 and predicted a protein with 691 amino acid residues (supplementary material Fig. S1A). When this protein sequence was initially compared with the zebrafish and mammalian genome using BLAST (approximate date October 2002), GA2692 showed homology to a human EST dubbed FLJ32150. Subsequent blast searches in 2003 showed that, the mouse and human HspA12B demonstrated a 70% identity to GA2692, human HspA12B and FLJ32150 were identical in their overlap regions, and GA2692 had a 30% identity to HspA12A (supplementary material Fig. S1A,B). A phylogenetic tree analysis also indicated that GA2692 evolved from the same ancestor as HspA12Bs in other species (supplementary material Fig. S1C). It is therefore likely that HspA12B is the mammalian orthologue of zebrafish GA2692. In added support of this relationship is the restricted expression of HspA12B to cultured endothelial cells (see below).

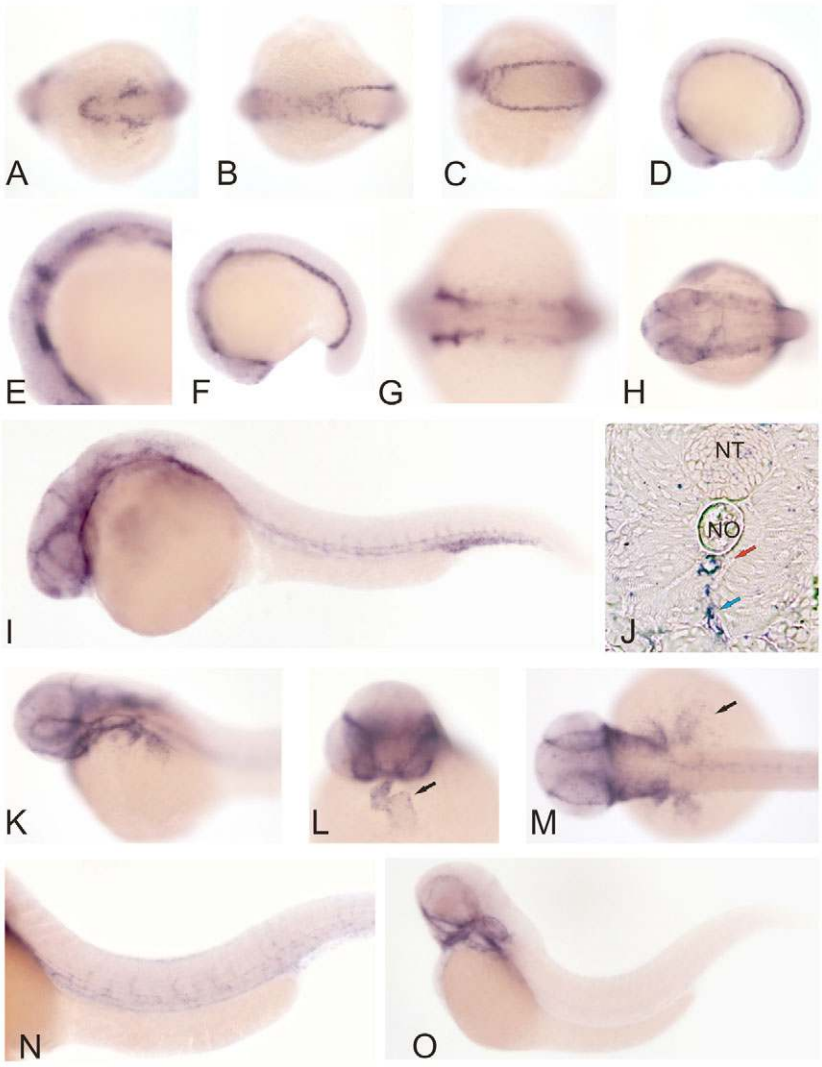

Fig. 1. HspA12B whole-mount in situ hybridization at different zebrafish developmental stages. (A-G) Middle somite stages. (A-C) Dorsal views of head, trunk and tail, respectively, showing staining in ventral hematopoietic and vasculogenic mesoderm. (D,E) Lateral (D) and enlarged lateral view (E) of head region showing expression in rhombomeres. (F) Lateral view showing expression in first somite. (G) Dorsal view of ear showing staining in the anterior part of the otic vesicle. (H-J) Embryos at 24 hpf, dorsal view of head region (H), lateral view of the whole embryo (I), JB4 cross section in the truck region of embryos at 24 hpf (J). Arrows point to arterial and venous structures. NT, neural tube; NO, notochord. (K-N) Embryos at 36 hpf. Enlarged lateral view of the head (K), front view showing staining in the heart (arrow) (L), dorsal view of the head region (M); arrow indicates duct of Cuvier. Lateral view of trunk (N) showing staining in both axial vessels and ISVs. (O) Lateral view of an embryo at 48 hpf.

Expression of HspA12B during embryonic development of zebrafish

A detailed characterization of HspA12B was carried out at different developmental stages. No expression of HspA12B was found before 10-somite stage. During the middle of somitogenesis (12 to 16 somite stage), expression was observed in ventral hematopoietic and vasculogenic mesoderm in both posterior and cephalic territories (Fig. 1A-D). Weaker expression was also observed in anterior telencephalon, diencephalon and hindbrain rhombomeres, probably in the ventral part of rhombomeres 3 and 5 (Fig. 1E), the first somite (Fig. 1F) and also the anterior part of the otic vesicle (Fig. 1G).

At 24 hpf, expression of HspA12B was mostly observed in vasculature (such as head, aorta, caudal vein, posterior cardinal

vein and intersegmental blood vessels) (Fig. 1H-J). Expression could also be found in telencephalon, anterior diencephalon, head mesenchyme, choroid fissure and heart (Fig. 1H,I).

At 36 hpf, expression was observed in head vasculature (Fig. 1K), heart (Fig. 1L, arrow head), duct of Cuvier (Fig. 1M, arrowhead), axial vasculature, intersegmental blood vessels (Fig. 1N), head mesenchyme (mainly around the eye and the otic vesicle) (Fig. 1K-M) and branchial arches (Fig. 1K). At 48 hpf, expression was restricted to splanchnocranium (otic placode, trabecula cranii, lower jaw). Expression decreased after 48 hpf.

Knockdown of HspA12B by antisense morpholino oligonucleotides (MOs)

Since an MO sequence targeting six bases upstream of the ATG start site (ATATTACAGGACTTTCACAGCCCGA) was derived against the region located six bases before the start codon, we expected that it would serve as a translation blocker. We therefore tested the potency and specificity of the HspA12B MOATG in an in vitro transcription and translation system. The HspA12B MOATG inhibited protein translation in a dose-dependent manner (Fig. 2A). However, no inhibiting effect from the corresponding mis-pairing control sequence for MOATG (MM) was observed even at 10 μM.

The knockdown of HspA12B using MO sequence targeting the third exon-intron junction to block the splicing of mRNA precursor (ATTTTAGAGGAGTTTCACACCCGGA) was also confirmed by reverse transcription-PCR (Fig. 2B). RNA was extracted from zebrafish embryos injected with various amount of MOs. The alternative splicing of mRNA caused by MOs3rd was verified by RT-PCR. Results showed that almost all mRNA was alternatively spliced after injection of 0.2 mM MOs3rd. A further increase in the concentration of MOs3rd can even reduce the total mRNA level.

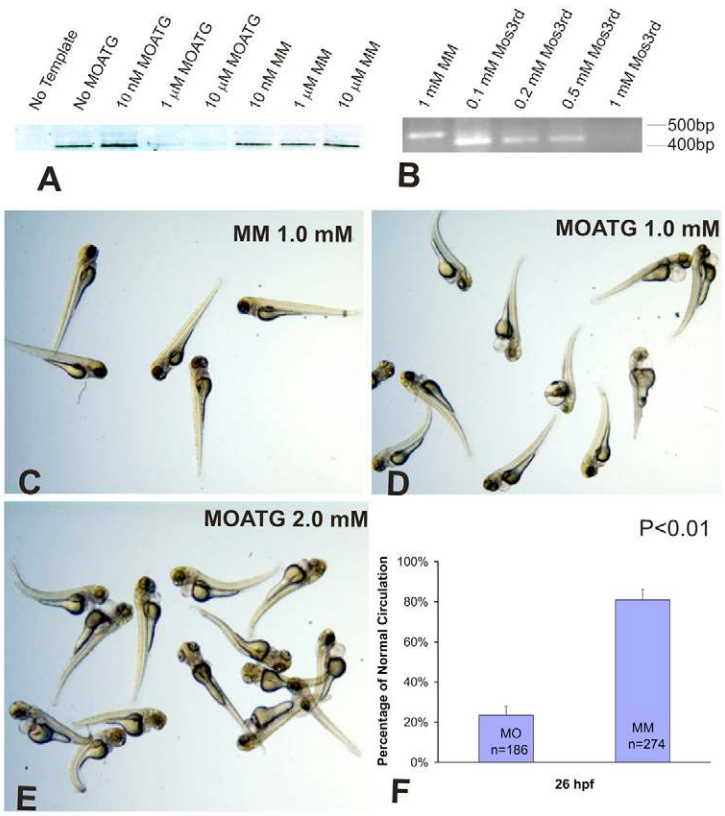

Fig. 2. Knockdown of HspA12B by MOs during zebrafish development. (A) In vitro transcription and translation in the absence of MOATG or in the presence of various concentrations of MOATG or MM, demonstrating the efficiency of MOATG in blocking the translation of HspA12B. (B) RT-PCR of zebrafish HspA12B from zebrafish embryos injected with various amounts of MOs3rd. (C-E) Embryos at 48 hpf injected with (C) 1.0 mM MM, (D) 1.0 mM or (E) 2.0 mM MOATG. (F) Percentage of normal circulation in morphants injected with 1.0 mM MOATG or MM at 26 hpf. Data are presented as the mean ± s.e.m. of three or more independent experiments; the difference between MM and MOATG was significant (P<0.01) as accessed by two tailed Student's t-test.

Knockdown of HspA12B causes vascular developmental defects in zebrafish

Zebrafish embryos were microinjected with HspA12B MOATG, MOs3rd and MM at 1 to 4 cell stage and examined for vascular defects at 24, 48 and 72 hpf. At different stages, embryos injected with MM had normal blood cell circulation in the axial vessels (dorsal aorta and posterior cardinal vein), the intersegmental vessels (ISVs), the dorsal longitudinal anastomotic vessels (DLAVs), the subintestinal vessels (SIVs) and the pectoral fin vessels. However, the majority of embryos injected with MOATG and MOs3rd exhibited slower trunk circulation and severely compromised circulation through the ISVs. The phenotype became more obvious as the concentration of MOATG and MOs3rd was increased. Embryos injected with MOATG and MOs3rd exhibited very similar phenotypes, although a higher dose was required for MOATG to show the same potency as MOs3rd. Table 1 shows the dose response of the circulation defects noticed for MOATG: 4.3% of embryos presented circulation defects in 0.5 mM MOATG-injected fish vs 41.5% and 60% in 1.0 mM and 2.0 mM MOATG-injected fish respectively. As the MOATG and MOs3rd concentration was increased, the following phenotypes were also noticed (Fig. 2C-E): (1) The total body length decreased; (2) the lumen of axial vessels including the dorsal aorta and axial vein was narrowed and short-circuiting of blood flow could be observed; (3) flow in the ISVs, SIVs and the vascular arch of the fin bud was disrupted; (4) blood cells accumulated in the tail vein plexus and/or common cardinal vein and; (5) pericardial edema was noticed in most fish (Fig. 2D,E).

Microangiography and alkaline phosphatase staining further demonstrate vascular defects in HspA12B morphants

To further investigate the vascular phenotypes in HspA12B morphants, we used microangiography with 0.02 μm fluorospheres and did alkaline phosphatase (AP) staining (which only stains endothelial cells) on MOATG- and MM-injected fish. Microangiography clearly demonstrated absence of circulation in ISVs in morphants and narrowed trunk vessels compared with controls (Fig. 3A,B). At 72 hpf, AP staining showed that SIVs and fin vessels also had defects to varying degrees depending on the concentration of MOATG injected, whereas there were no observable vessel defects in MM-

Table 1. Live observation in MOATG-injected fish

	Wild type	0.5 mM MO	1.0 mM MO	2.0 mM MO
Embryos injected	42	47	41	35
Slow circulation	0 (0%)	2 (4.3%)	11 (26.8%)	12 (34.3%)
No circulation	0 (0%)	0 (0%)	6 (14.6%)	9 (25.7%)
Total circulation defect	0 (0%)	2 (4.3%)	17 (41.5%)	21 (60%)

Different concentrations of MOATG were injected into embryos at 1 to 4-cell stages. The circulation was examined at 48 hpf. Numbers in brackets give percentage of affected embryos in total embryos examined.

injected fish. As the concentration of MOATG was increased, the defects in these two vessels increased (Fig. 3C-H). In the 0.5 mM group, the percentages with defects of SIVs and fin vessels were 8.89% and 17.78%, respectively (Fig. 3I,J). In the group injected with 1.0 mM MOATG, percentages of defects of SIVs and fin vessels were 80% and 85%, respectively. In the group injected with 2.0 mM MOATG, percentages of defects of SIVs and fin vessels were 82.76% and 89.66%, respectively.

Knockdown of HspA12B in the [*Tg(fli1:EGFP)*^{y1}] zebrafish line disrupts the angiogenic formation of ISVs and DLAVs

These results pointed to multiple vascular defects in the HspA12B morphants. Next, to assess whether the defects seen could be ascribed to the absence of endothelial cells in the HspA12B morphants, we carried out the knockdown experiments in the [*Tg(fli1:EGFP)*^{y1}] zebrafish line, in which virtually all ECs and their angioblast precursors are highlighted by the robust expression of EGFP driven by a 15 kb fli-1 promoter (Isogai et al., 2003; Lawson and Weinstein, 2002). The use of these fish allowed us to monitor vascular development in real time by fluorescent microscopy.

After injecting MOsATG, early vasculogenesis, the de novo formation of major trunk vessels by co-migration and coalescence of angioblast progenitor cells originating in the trunk lateral mesoderm (Risau and Flamme, 1995), was largely unaffected in the morphants in comparison with wild-type fish (data not shown). However, the formation of ISVs and DLAVs, an angiogenic process that involves the sprouting and migration of ECs from the axial vessels, was disrupted in the HspA12B morphants. At 27 hpf, the EC sprouts appeared sporadically along the longitude of the HspA12B morphants, in contrast to their blossoming in the control embryos (Fig. 4A,B). At 36 hpf, an elaborate network of ISVs and DLAVs was clearly visible in control embryos, whereas the dorsal part of this network was completely absent in the morphants, even

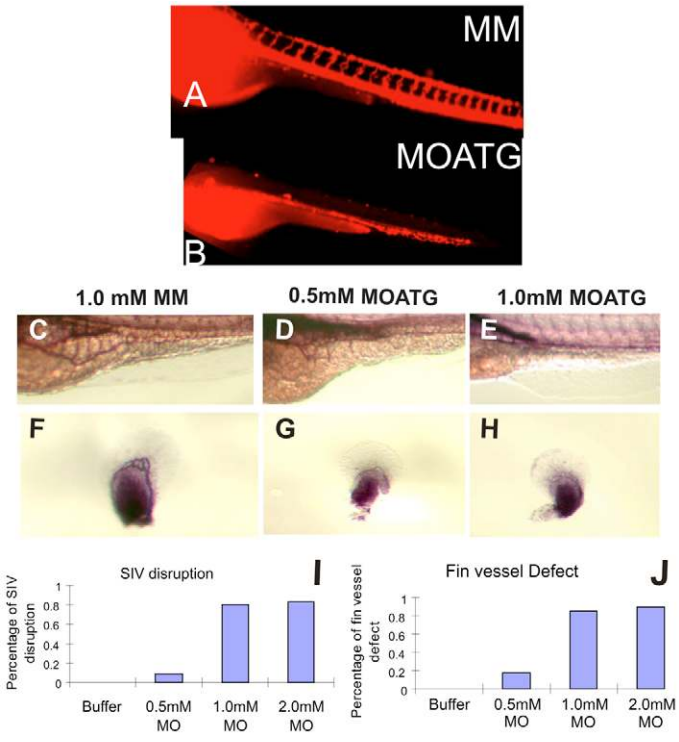

Fig. 3. Vascular phenotypes in morphants defined by microangiography and AP staining. (A,B) Angiogram of fish injected with 1 mM MM (A) or MOATG (B) at 48 hpf. (C-J) AP staining and statistical analysis of morphants treated with various concentrations of MM or MOATG. (C-E) SIVs. (F-H) Pectoral fin vessels. (I,J) Statistical analysis. (A,C,F) Embryos injected with 1.0 mM MM. (D,G) Embryos injected with 0.5 mM MOATG. (B,E,H) Embryos injected with 1.0 mM MOATG.

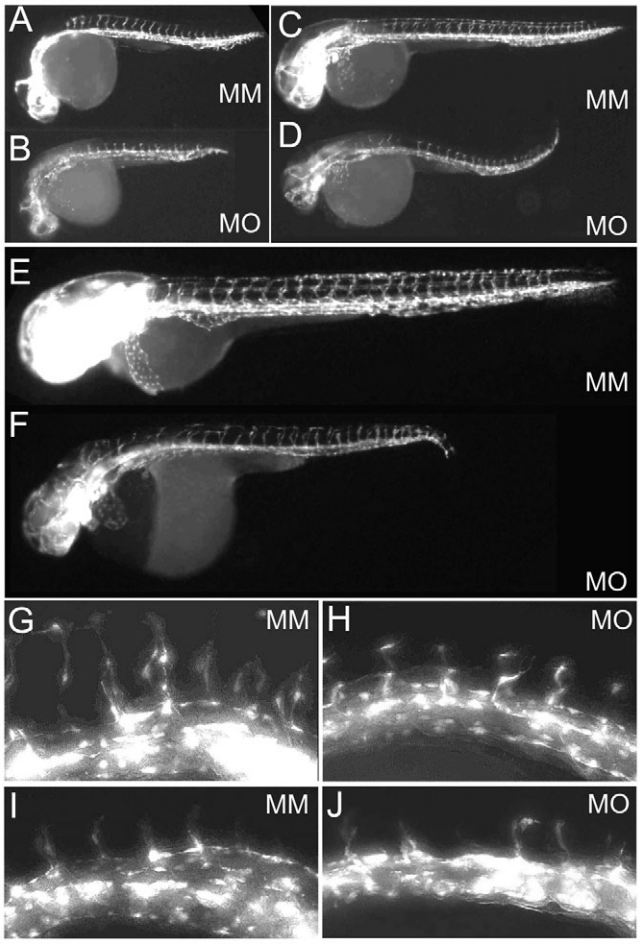

Fig. 4. Impaired angiogenic processes revealed by knockdown of HspA12B in the [*Tg(fli1:EGFP)*^{y1}] zebrafish line. (A,C,E,G,I) Morphants injected with 1 mM MM. (B,D,F,H,J) Morphants injected with 1 mM MOATG. (A,B,G,H) Morphants at 27 hpf. (C,D) Morphants at 36 hpf. (E,F) Morphants at 54 hpf. (I,J) Morphants at 24 hpf. In panels G-J, the rostral is to the left.

Table 2. Effects of MOs on different vessels

Vessel type	0.1 mM MOs3rd	0.2 mM MOs3rd	1 mM MOATG	1 mM MM
ISVs	0	0	71.4	14.3
DLAVs	0	35.3	85.7	14.3
Parachordal sprouts	4.2	64.3	85.7	14.3

Effects of MOs on the reduction of the dorsal part of ISVs, parachordal endothelial cell sprouts and DLAVs in the [*Tg(fli1:EGFP)*^{y1}] zebrafish line at 48 hpf, analysed by fluorescence microscopy. Data are presented as the percentage of affected embryos of total embryos examined.

14 hours after the initial sprouting (Fig. 4C,D). Therefore, this difference is unlikely to merely represent a delay in an otherwise largely normal developmental program. At 54 hpf, a small percentage of these ECs remained exactly where they were at 36 hpf; some ECs branched horizontally at the midline and connected to each other; others did sprout dorsally during this time but followed distorted paths, resulting in fragmentary DLAVs (Fig. 4E,F). This was observed in 85.7% of embryos injected with MOATG. These ISVs and DLAVs were not functional, as previously demonstrated by microangiography (Fig. 3A,B) and visualization of the circulation (data not shown). Furthermore, sprouts of parachordal endothelial cells were dramatically reduced in most zebrafish embryos injected with MOATG or MOs3rd (Table 2).

To examine more closely the ISV sprouting from DA, we used live time-lapse analysis to track the sprouting endothelial cells during formation of the primary ISV network. In MM injected embryos, most ISVs extended slightly rostrally and then caudally after crossing the transverse myoseptum, potentially following the chevron-like contours of the somites, before reaching the dorso-lateral surface, where tubes from adjacent ISVs fused to form the DLAVs. Movies from embryos injected with MOATG showed that the axial vessels did extend rostrally but then made a sharp caudal turn. In fact, most ISVs formed preliminary T-shape structure prior to reaching the dorso-lateral surface when compared to age-matched MM-injected embryos (Fig. 4G,H and supplementary material Movie 1). Moreover, the rostral-caudal coordinated timing of ISV sprouts was disturbed in the MOATG-injected embryos (Fig. 4I,J and supplementary material Movie 2). Taken together, the time-lapse results and the spectrum of ISV defects in other assays suggested that, in general, reduced HspA12B levels in endothelial cells might render them incompetent to respond spatially and temporally to cues from the surrounding environment.

The specific expression of HspA12B in vasculature and its importance in angiogenesis during zebrafish early development prompted us to investigate the function of its human orthologue. We began by first assessing HspA12B expression levels in multiple cell lines.

Human HspA12B is specifically expressed in endothelial cells

Northern blot analysis using the coding region of human HspA12B as a probe showed that HspA12B was present in human umbilical vein endothelial cells (HUVECs), and not detectable in fibrosarcoma cells (HT1080 cells), human embryonic kidney epithelial cells (HEK 293 cells), human colon cancer cells (DLD1 cells), ovarian cancer cells

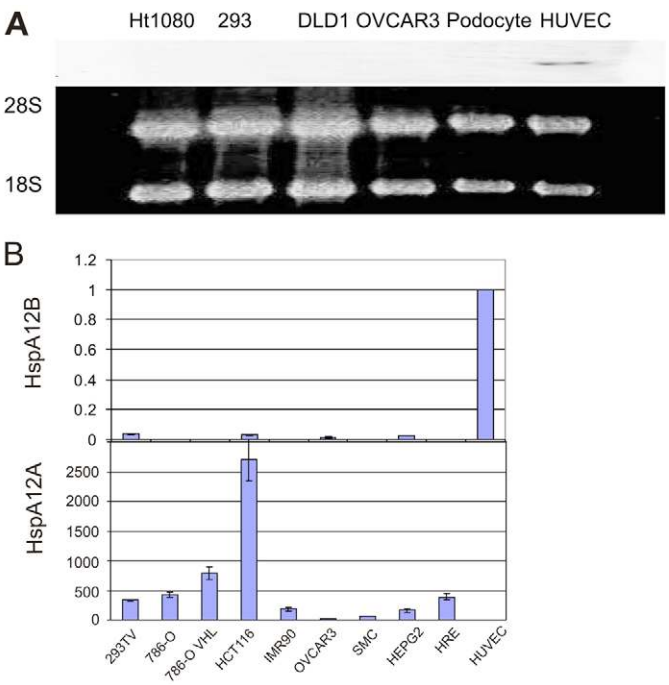

Fig. 5. Expression profile of human HspA12A and HspA12B in human cell lines. (A) Detection of HspA12B mRNA in human cell lines by northern blot. Signal is evident only in the HUVEC lane (upper panel), 28S and 18S staining is shown as equal loading control (lower panel). (B) Comparison of HspA12A and HspA12B mRNA levels in cell lines using real-time PCR. Data from two independent experiments were normalized with the expression levels in HUVECs and are presented as the mean ± s.e.m.; the difference of expression levels between HUVECs and other cell lines were all significant (P<0.05) as tested by two tailed Student's t-test.

(OVCAR3 cells) and podocytes (Fig. 5A). Since HspA12A is closely related to HspA12B, we decided to compare the expression of HspA12B and HspA12A in a broader spectrum of cell lines by real-time PCR, which is more quantitative than northern blot analysis. Similar to the results of our northern blot analysis, the expression of HspA12B was highly specific to HUVECs (Fig. 5B), with the expression level 26-fold higher compared with the second highest expression cell line (293TV). Interestingly, the expression level of HspA12A in HUVECs was the lowest among all cell lines we checked. The second lowest expressor were OVCAR3 cells, still 24.5 fold higher than that of HUVECs. These results were consistent with the endothelial specific expression pattern of HspA12B in zebrafish, and also suggested that the function and regulation of HspA12A and HspA12B are probably distinct, although they are similar in primary sequence. Given the specific expression of HspA12B in endothelial cells, we proceeded to investigate its role in a number of angiogenesis assays in vitro.

Knockdown and overexpression of HspA12B in HUVECs

To knockdown the expression of HspA12B in HUVECs, four siRNAs (si1, si2, si3 and si4) and a negative control siRNA (NC) were tested by co-transfecting them with pCS2+-HspA12B/C-FLAG at a ratio of 50:1 in HEK 293 cells; lysates were collected 48 hours post-transfection and resolved by SDS-PAGE. si1 and si3 knocked down the expression of

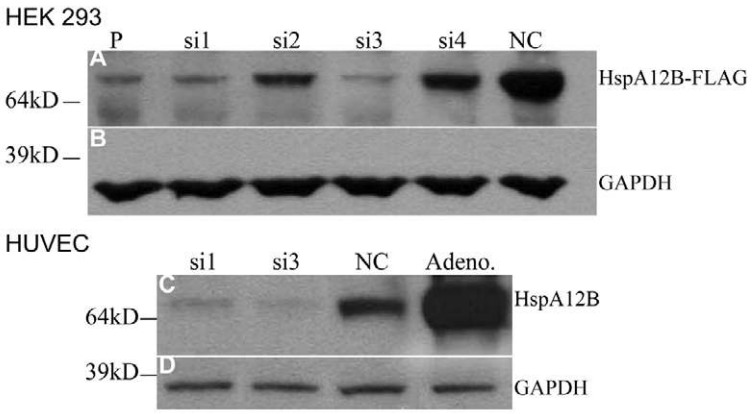

Fig. 6. Knockdown and overexpression of HspA12B. (A) HEK 293 cells cultured in six-well plate were transfected with 0.1 μg pCS2+-HspA12B-Flag and various siRNAs at 62.5 nM final concentration. Cell lysates were collected after 48 hours and the expression level of HspA12B-Flag was checked by western blot using anti-FLAG antibody. P, pool of si1, si2, si3 and si4. (B) GAPDH loading control for (A). (C) HUVECs were transfected with si1 and si3 at 62.5 nM final concentration in six-well plates and endogenous HspA12B expression was examined after 48 hours by western blot using Ab4112 antibody; Lane 4 was loaded with lysate from HUVECs infected with HspA12B-C-FLAG adenovirus. (D) GAPDH loading control for (C).

HspA12B/C-FLAG to 13.8% and 8.2%, respectively, compared with that of NC, whereas si2 and si4 were less effective (Fig. 6A,B). Therefore, si1 and si3 were tested further in HUVECs. After transfecting these two siRNAs into HUVECs, si1 and si3 were – as expected from the transfection data in HEK293 cells – found to reduce endogenous expression by over 85% (Fig. 6C,D), as assessed with a polyclonal antibody against HspA12B (Steagall et al., 2006). Infection of HUVECs with HspA12B/C-FLAG adenovirus at a multiplicity of infection (MOI) of ~100 increased the expression level by approximately fivefold compared with control.

HUVEC migration is augmented by overexpressing HspA12B and inhibited by HspA12B siRNAs in vitro

Since angiogenesis is a composite process in which cell migration plays a central role, we used a HUVEC migration assay to test the role of HspA12B in this process. We found that cells overexpressing HspA12B via adenoviral-mediated gene transfer migrated about three times faster than control cells infected with empty control adenovirus (Fig. 7A). Next, we repeated our experiments under stimulation by vascular endothelial growth factor (VEGF), a potent and well-studied pro-migratory agent for endothelial cells. In the migration assay with 10 ng/ml VEGF, HspA12B-augmented HUVEC migration was only 33% higher compared with that of HUVECs infected with empty virus (Fig. 7A), suggesting that HspA12B induced downstream signaling pathways might overlap with those induced by VEGF. Conversely, the number of migrated cells from HUVECs transfected with si1 and si3 under VEGF stimulation was about 40% of that noticed with cells transfected with NC (Fig. 7B), suggesting that HspA12B influenced VEGF signaling. Of importance, the use of si1 and si3 gave a similar phenotype, demonstrating that the phenotype was likely to be due to the knockdown of HspA12B expression. si1 and si3 also had some effect in blocking baseline migration in DMEM supplemented with 0.5% serum, suggesting that HspA12B may influence the 'basal' migratory machinery (Fig. 7B).

To further study the effect of HspA12B on migratory responses, we used a wound healing assay to compare the motility of the HUVECs infected with sense adenovirus or transfected with siRNAs. Infected or transfected HUVECs

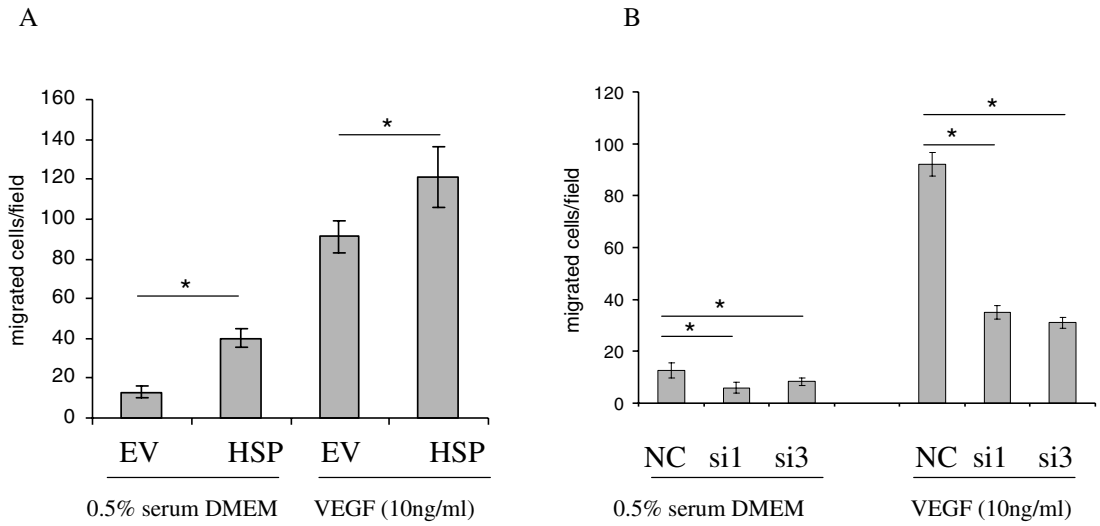

Fig. 7. Effect of HspA12B on VEGF-induced HUVEC migration. HUVECs were infected with empty control or HspA12B adenoviruses and migration assay was done in DMEM supplemented with 0.5% serum or DMEM supplemented with 0.5% serum and VEGF (10 ng/ml) in the lower chamber. HUVECs were transfected with NC, si1 and si3. Data from three experiments are shown as the mean ± s.d. All comparison were tested for statistic significance using two-tailed Student's *t*-test. **P*<0.05.

were grown to confluence on six-well plates, and wounds were made in the cell monolayer. Endothelial growth medium 2 (EBM-2) supplemented with 1% serum (Fig. 8A,B) or EBM-2 supplemented with 1% serum and VEGF (10 ng/ml) (Fig. 8C-F) were used in the experiments. HspA12B strongly promoted wound closing in either conditions (Fig. 8A-D) and si1 and si3 transfection decreased wound closing (Fig. 8E,F). These data were consistent with our migration assay results.

Blocking of tube formation by siRNA transfection into HUVECs

The tube-formation assay measures a number of functions of endothelial cells including cell survival, cell migration, the ability to connect to other endothelial cells and lumen formation. In this assay, we found that NC-transfected HUVECs form well-connected tube-like structures, whereas si1 and si3 transfected HUVECs barely formed tube-like structures, resembling the effect seen with potent antiangiogenic molecules (Fig. 9), and being consistent with our zebrafish phenotype.

HspA12B is necessary for Akt phosphorylation in endothelial cells

To get more insight into the function of HspA12B, we studied the effects of HspA12B siRNAs (si1 and si3) on Akt phosphorylation, known to be modulated by VEGF (Shiojima and Walsh, 2002). We found that HUVECs transfected with si1 and si3 showed diminished phosphorylation levels of Akt in the presence of VEGF, and even under normal serum conditions. By contrast, there was no significant change in the level of total Akt protein (Fig. 10A). To ask whether diminished Akt phosphorylation accounts for the effect on HUVEC migration of HspA12B siRNAs, we attempted to rescue this phenotype with a constitutively active Akt (myr-Akt). Indeed, the inhibitory effects of HspA12B siRNAs were abolished with myr-Akt (Fig. 10B).

Discussion

The identification of HspA12B as an endothelial specific gene crucial for angiogenesis (in vivo) demonstrates the power of using the zebrafish for functional gene discovery. Our whole-mount in situ screen enabled us – without relying on any previous knowledge – to identify new genes that are specifically expressed in vasculature. Benefiting from various attributes of zebrafish vasculature development (e.g. transparency of the embryo, development of circulation in the first 48 hpf) and the availability of transgenic fish in which EGFP is selectively expressed in endothelial cells (Isogai et al., 2003; Lawson and Weinstein, 2002), we could immediately gain insight into the function of these genes in vivo by using morpholino oligonucleotides as a tool for loss-of-function analysis. These in vivo results could then be further dissected and signaling pathways studied via in vitro assays in primary endothelial cells such as HUVECs, after identification of the HspA12B human orthologue using bioinformatics tools. By combining the advantages of both in vivo and in vitro systems, we have demonstrated a functionally important role for HspA12B in endothelial biology.

While this work was in progress, another study pointed to the endothelial cell specific expression of HspA12B. Durr et al. described HspA12B as one of about 450 proteins identified by multidimensional protein-identification technology in endothelial cells isolated from rat lungs and in cultured rat lung microvascular endothelial cells (Durr et al., 2004). More recently, a search for HspA12B in GENSAT, a new transgenic mouse resource that has been integrated into the Entrez NCBI database, showed that HspA12B was expressed in endothelial capillaries in the brain. A detailed characterization of the expression of HspA12B in these transgenic mice will be presented elsewhere and shows that it is expressed in

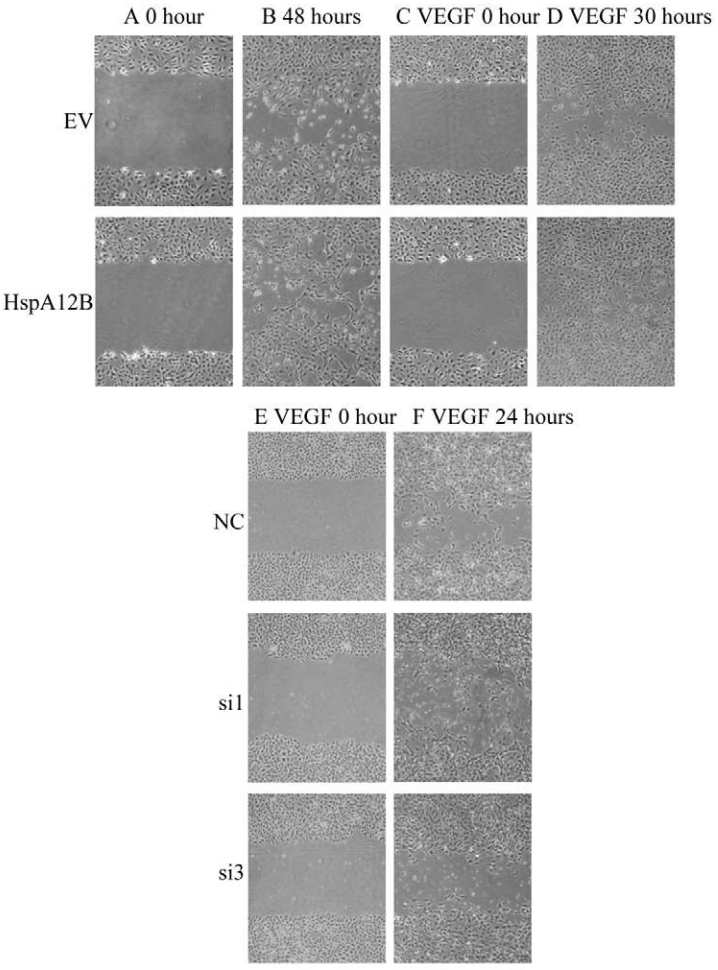

Fig. 8. Wound healing assays using HUVECs. (A,B) HUVECs infected with empty control and sense adenoviruses were grown to confluence. Wounds were made using 200 μl pipette tips in the cell lawn 48 hours after infection and media was changed to EBM-2 supplemented with 1% serum after the injury. Pictures were taken at 0 and 48 hours. (C,D) HUVECs infected with the same adenoviruses were grown to confluence. After making the wound, EBM-2 supplemented with 1% serum and VEGF (10 ng/ml) was added. Pictures were taken at 0 and 30 hours post injury. (E,F) HUVECs transfected with NC, si1 and si3 were grown to confluence and wounds were made in the cell monolayer 48 hours after transfection. EBM-2 supplemented with 1% serum and VEGF (10 ng/ml) was added. Pictures were taken at 0 and 24 hours post injury. Representative pictures were shown from at least three independent experiments.

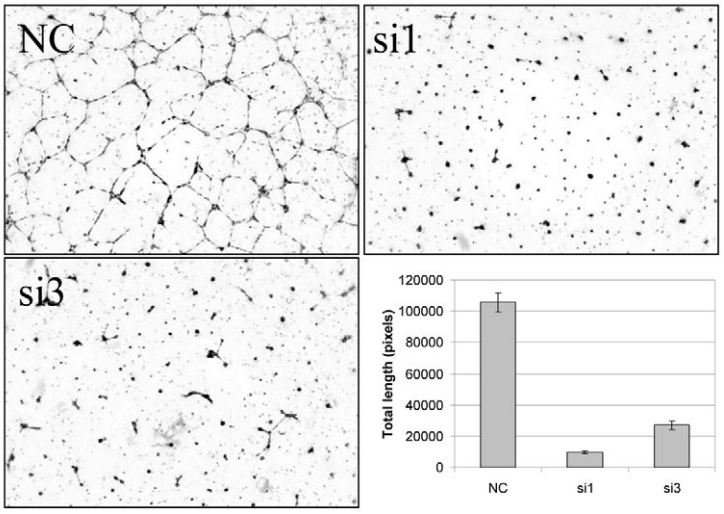

Fig. 9. HUVEC tube formation assay. HUVECs were transfected with NC, si1 and si3. After 48 hours, cells were trypsinized and resuspended in EBM-2 supplemented with 2% serum, and 4×10^4 cells were added to each well of a 48-well tissue culture plate with 100 μl solidified growth-factor-reduced Matrigel. Pictures were taken at 24 hours. Representative pictures from five independent experiments are shown. Quantitative data are shown as the mean ± s.e.m. All difference between groups were statistically significant (P<0.05), tested by two tailed Student's t-test.

endothelial cells of arteries, veins and capillaries in all organs examined (Steagall et al., 2006). Collectively, these data, including ours from fish, strongly suggest that HspA12B is a gene that is highly specific for endothelial cells.

The above studies address only expression and do not speak to the function of HspA12B. We have addressed this question, first in vivo in fish and then in vitro in HUVECs and shown that the angiogenic potency of endothelial cells was greatly impaired in the absence of or with diminished expression of HspA12B. Knockdown of HspA12B expression using morpholino oligonucleotides in zebrafish compromised the sprouting of ISVs, the formation of intact DLAVs, and hampered the formation of SIVs and pectoral fin vessels; whereas knockdown of HspA12B in HUVECs by siRNAs led to inhibition of wound healing, migration and tube formation.

Knockdown of HspA12B reduced the phosphorylation of Akt under three different conditions but had little effect on the total level of Akt. Akt phosphorylation is one of the key events transducing multiple angiogenic signals, including those initiated by VEGF, Angiopoietin-1 and FGF-2. The attenuation of Akt phosphorylation could be one of the mechanisms by which knockdown of HspA12B expression blocks angiogenesis. Our results also suggest that reduction of phosphorylated Akt could at least account for the inhibitory effect of HspA12B siRNAs on the migration of HUVECs, because overexpression of myr-Akt, a constitutively active form of Akt could overcome these effects. However, we did not see such a rescue in the tube-formation assay (data not shown), suggesting the existence of additional targets by which HspA12B affects tube formation.

We do not yet know whether HspA12B is a heat-inducible protein or what else induces its expression. Intriguing is the fact that it is rather uniquely expressed in endothelial cells, because Hsps are typically not cell or tissue specific, suggesting that it may play a unique role in protecting endothelium from 'toxic' insults. For example, Hsp synthesis is known to be induced in all cell types in the blood vessel wall, including endothelial cells, upon exposure to environmental stress, heat, hormones, reactive oxygen species and sodium arsenite (Snoeckx et al., 2001). However, HspA12B is

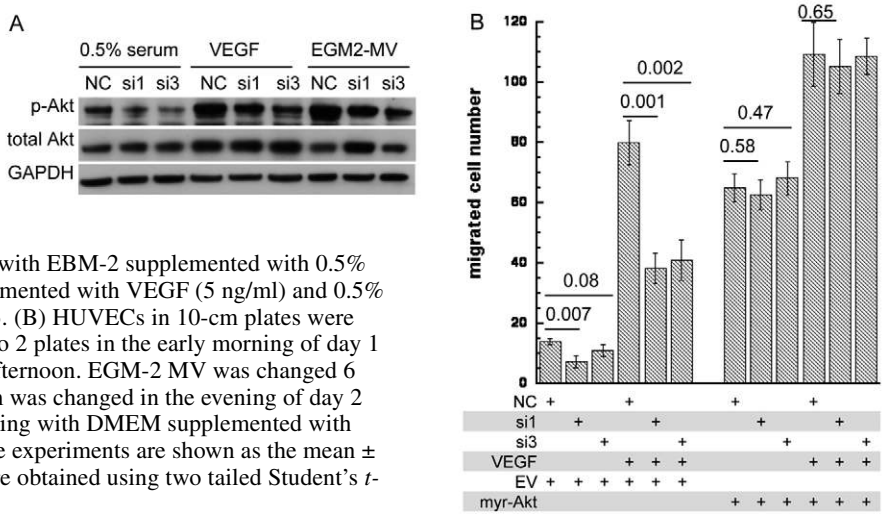

Fig. 10. Western blot analysis of Akt phosphorylation in cells transfected with siRNAs, and HUVEC migration rescue experiment with myr-Akt. (A) HUVECs in six-well plates were transfected with NC, si1 and si3 on day 0, split on day 1, serum-starved with EBM-2 supplemented with 0.5% serum on day 2 and stimulated with EBM-2 supplemented with VEGF (5 ng/ml) and 0.5% serum or with EGM-2 MV for 30 minutes on day 3. (B) HUVECs in 10-cm plates were transfected with NC, si1 and si3 on day 0, split onto 2 plates in the early morning of day 1 and infected with myr-Akt adenovirus in the late afternoon. EGM-2 MV was changed 6 hours later, EBM-2 supplemented with 2.5% serum was changed in the evening of day 2 and migration assay was done on day 3 by stimulating with DMEM supplemented with VEGF (10 ng/ml) and 0.5% serum. Data from three experiments are shown as the mean ± s.d. All indicated P values for the comparisons were obtained using two tailed Student's t-test.

constitutively expressed in endothelial cells, distantly related to the Hsp70 family and, as yet, we do not know whether its expression can be modulated by heat shock or other insults. Aside from their roles as molecular chaperones and stress protecting proteins, Hsps are also being recognized as active components constitutively involved in many cellular processes. All proteins need to constantly change their conformation to be properly functional, often resulting in transient exposure of surfaces similar to those found in denatured proteins. By recognizing and associating with these surfaces to prevent undesirable protein interactions, Hsps facilitate many cellular processes, including cell signaling pathways. Future studies will aim at identifying client proteins for HspA12B, some of which may be endothelial specific whereas others may be more generally expressed signaling molecules, and defining how and whether it promotes 'endothelial health' in general and the angiogenic response in particular; they will promise a deeper understanding of its function in endothelial biology. For example, the ability to induce HspA12B expression may promote endothelial health and therefore be of importance in the treatment of disorders in which there is evidence of endothelial dysfunction, e.g. atherosclerosis (in which HspA12B expression was first noted in macrophages) (see Han et al., 2003), sepsis or preeclampsia. Similarly, inhibition of HspA12B expression or action (e.g. by drugs that inhibit the binding of ATP to the putative ATP binding site of HspA12B) may benefit patients with dysregulated angiogenesis, like, among others, in cancer or in ocular neovascularization processes, especially if it is shown that HspA12B expression is augmented in these conditions. Finally, serum antibodies to HspA12B or the serum level of shed HspA12B might reflect the functional state of endothelium in humans.

In conclusion, the present study demonstrates that the HspA12B is selectively expressed in endothelial cells and is essential for both normal zebrafish vascular development in vivo and multiple endothelial cell functions in vitro.

Materials and Methods

Isolation of cDNA clone

GA2692 was identified by whole-mount in situ hybridization (WMISH) screen (Galloway et al., 2005) and was isolated from an adult zebrafish kidney cDNA library (J. Rast, Children's Hospital, St Petersburg, FL).

Zebrafish lines and maintenance

Adult zebrafish were maintained as described (Westerfield, 2000). Developmental stages were determined by embryo morphology and hpf (Kimmel et al., 1995). Embryo medium was supplemented with 0.003% 1-phenyl-2-thiourea (Sigma) before embryos reach 24 hpf to prevent melanin formation.

Whole-mount in situ hybridization

Whole-mount in situ hybridization was carried out as described (Jowett and Lettice, 1994; Thisse et al., 2004). For histological analysis, specimens were fixed in 4% paraformaldehyde overnight at 4°C, dehydrated with ethanol, and embedded in JB-4™ resin (Polysciences, Inc., Warrington, PA). Specimens were sectioned at 6 μm using a Jung Supercut 2065 microtome and examined with a Nikon Optiphot 2 Microscope.

Antisense morpholino oligonucleotides: sequence and injection

Morpholino antisense oligonucleotides (MOs) were designed and synthesized by Gene Tools LLC., Philomath, OR. The sequences are, 5′-ATATTACAGGACTTTCACAGCCCGA-3′ (MOATG, MO targeting six bases upstream of the ATG start site), 5′-ATTTTAGAGGAGTTTCACACCCGGA-3′ (MM, the corresponding mispairing control for MOATG, the five mismatched bases are underlined) and 5′-ACAGACATAAATACCTCATCATGTG-3′ (MOs3rd, MO targeting the third exon-intron junction to block the splicing of mRNA precursor). Solutions were prepared and injected as described (Nasevicius and Ekker, 2000) using a gas driven microinjector (Pico-Injector, PL1-90, Harvard Apparatus).

In vitro transcription and translation

The TNT® quick coupled reticulocyte lysate system (Promega) was used according to the manufacturer's protocol with modifications. In a 12.5 μl reaction, 0.25 μg of pBK-CMV-HspA12B and different concentrations of MOATG and MM (0 nM, 10 nM, 1 μM and 10 μM final concentration) were added to the TNT Master Mix, containing all of the required components for in vitro transcription and translation plus ^{35}S-labeled methionine, and incubated at 30°C for 90 minutes. S^{35}-labeled proteins were visualized by autoradiography following separation on a 4-15% SDS-PAGE.

Reverse transcription-PCR of HspA12B fragments from zebrafish embryos

Following collection of embryos 48 hours after injection of various concentrations of MOs, total RNA was extracted using the RNeasy™ mini kit (Qiagen). Reverse transcription was performed according to SuperScript™ III first-strand synthesis system for RT-PCR using oligonucleotide dT primer (Invitrogen). PCR was carried out using Platinum® Taq DNA polymerase (Invitrogen). Forward and reverse primers were 5′-GCTGTGAAAGTCCTGTAATA-3′ and 5′-AAAGTATAGCCA-ATGTCTGG-3′, respectively.

Endogenous alkaline phosphatase (AP) staining

Whole-mount AP staining was carried out essentially according to a published protocol (Habeck et al., 2002).

Microangiography

Microangiography was performed as described (Weinstein et al., 1995) except that 0.02 μm Fluorospheres® with red fluorescence (Invitrogen) in 1% bovine serum albumin (BSA) were injected into the fish.

Time-lapse analysis

Movies were made as described in Bedell et al. (Bedell et al., 2005) except that *Tg(fli1:EGFP)*^{y1} embryos were used.

Northern blot analysis

Total RNA was extracted from different cell lines using RNeasy mini kit (Qiagen). RNA (10 μg) was subjected to northern blotting. The full-length human HspA12B coding region was PCR amplified (Advantage™ GC cDNA PCR kit from Clontech) from a human umbilical vein endothelial cell (HUVEC) reverse transcription product using primers: 5′-ACAGGATCCACCATGTTGGCTGTCCCGGAGATG-3′ and 5′-TCAGTTGGAAAGAAAGTCGATGGA-3′, and used as a probe after purification. A ^{32}P-labelled probe was generated using Prime-it® II random primer labeling kit (Stratagene). It was added to ExpressHyb™ rapid hybridization buffer (Clontech) and the blot was incubated for 3-4 hours at 65°C and then washed and autoradiographed.

Real-time PCR analysis

Specific sets of primers and Taqman® probes were designed by using Primer Express (Applied Biosystems) and synthesized by GenScript, Piscataway, NJ. The primer and probe sequences for human HspA12B were 5′-CTTCTTCAGG-GAGCACGCC-3′, 5′-TGTCCTTCTCTGGCAGCGA-3′ and FAM-5′-TCAGGA-GCTGAGGGAGCAGAGCCC-3′-TAMRA. The sequences for HspA12A (another gene highly homologous to HspA12B) were 5′-CAGGAATAACGCCTCTGTCC-3′, 5′-CACCACGAGAAATGACTGCT-3′ and FAM-5′-CCCTCCCATATTGTGA-ACGACACTGA-3′-TAMRA. Human glyceraldehyde-3-phosphate dehydrogenase (GADPH) primers (Applied Biosystems) were included in all reactions as an endogenous control. The RT-PCR reactions were performed on an Applied Biosystems 7500 RT-PCR system using Taqman® one-step RT-PCR master mix (Applied Biosystems). All data were analyzed by comparative C_t using the 7500 system SDS software (Applied Biosystems).

Polyclonal antibody against HspA12B

An anti-HspA12B polyclonal antibody, AB4112, was generated by immunizing rabbits with a synthesized peptide derived from mouse HspA12B with the following amino acid sequence, CVDVSTNRSVRAAIDFLSN. Detailed generation, purification and validation of this antibody is described elsewhere (Steagall et al., 2006).

Plasmid construction, adenovirus amplification and HUVEC infection

Full-length human HspA12B cDNA with a FLAG® tag was amplified using Advantage™ GC cDNA PCR kit (Clontech) from a HUVEC reverse transcription product using forward primer 5′-ACAGGATCCACCATGTTGGCTGTCCCGG-AGATG-3′ and reverse primer 5′-AAACTCGAGTCACTTATCGTCGTCATCC-TTGTAATCGTTGGAAAGAAAGTCGATGGA-3′. The PCR product was digested

with *BamH*I and *Xho*I and ligated into the pCS2+ expression vector, designated as pCS2+-S8 and confirmed by sequencing. The gene was further subcloned into the pShuttle-CMV vector by *BamH*I and *Xba*I digestion. Adenoviral recombinants were obtained using BJ 5183 AD-1 electrocompetent cells (Stratagene). Adenoviruses were amplified using QBI-HEK293A cells (QBiogene, Morgan Irvine, CA). Amplification, CsCl purification and virus storage were done as described (He et al., 1998) and viral titers were determined using Adeno-X™ Rapid Titer Kit (BD Biosciences). HUVECs (Cascade Biologics, Inc. Portland, OR) cultured in six-well tissue culture plates to 60% confluency were infected with adenoviruses for 6 hours at which point fresh EGM2™-MV medium (Cambrex) was added and cells were incubated for 24 to 48 hours prior to further experiments.

The constitutively active adenoviral Akt construct was a gift of Kenneth Walsh (Boston University) (Fujio and Walsh, 1999), which contains the Src myristoylation sequence fused in-frame to the N terminus of the HA-Akt (wild type) coding sequence that targets the fusion protein to the membrane. Virus amplification and purification were done as above.

siRNAs and transfection

All siRNAs (sequences shown below) against human HspA12B were obtained from Dharmacon. Silencer® negative control number1 siRNA (NC) was obtained from Ambion, Inc. Lipofectamine™ 2000 (Invitrogen) was used to transfect siRNAs into HEK 293 cells (final concentration 62.5 nM) in six-well plates and HUVECs cultured in six-well plates or 10-cm plates as suggested in the manual.

The sense sequences of the siRNAs are: siGENOME™ duplex 1 (si1), CCACGGAUCUCACCUUGAAUU; siGENOME™ duplex 2 (si2), CGACUUU-CUUUCCAACUGAUU; siGENOME™ duplex 3 (si3), GGGACUGGCUCUACU-UCGAUU; siGENOME™ duplex 4 (si4), CCAGCUAGAGGCAGUAAAUUU.

Western blot analysis

Protein lysates were collected from HUVECs or HEK293 cells using RIPA buffer with protease inhibitor cocktail complete mini tablets (Roche). For protein phosphorylation studies, additional phosphatase inhibitor cocktail 1 and 2 from Sigma Aldrich was added to the RIPA buffer. HUVECs were serum starved in endothelial growth medium 2 (EBM-2, Cambrex) supplemented with 0.5% serum for 24 hours before stimulation with VEGF (10 ng/ml) in 0.5% serum EBM-2 or EGM™-2 MV (Cambrex). Protein concentration was measured using BCA protein assay reagents from Pierce. Proteins were loaded onto Novex® 4-12% Bis-Tris gel or 3-8% Tris-acetate gel (Invitrogen) and transferred onto an Immobilon-P PVDF Transfer membrane (Millipore). Anti-Akt (pS473) rabbit monoclonal antibody was obtained from Abcam; antibody against total Akt1/2 rabbit polyclonal IgG was from Santa Cruz Biotechnology; monoclonal antibody against GAPDH was obtained from Chemicon International. The horseradish-peroxidase-coupled secondary antibodies were from GE Healthcare and SuperSignal™ chemiluminescent substrates (Pierce) were used for visualization.

Migration and wound healing assays

Migration assay was done as previously described (Seth et al., 2005). HUVECs infected with adenovirus or transfected with siRNAs were grown in six-well tissue culture plates and a wound of defined size was made in the confluent cell monolayer with a pipette tip. Phase-contrast micrographs were used to assess wound closure at 0, 16 and 60 hours.

Tube-formation assay

The tube-formation assay and quantification was performed as previously described (Merchan et al., 2003).

We thank Brant Weinstein for his kind gift of the *Tg(fli1:EGFP)*^{y1} transgenic fish, Kenneth Walsh for the myr-Akt adenovirus, and Sonia Sinha for zebrafish maintenance and whole-mount in situ hybridization. This work was supported by seed funds from the Beth Israel Deaconess Medical Center.

References

Artigues, A., Iriarte, A. and Martinez-Carrion, M. (1997). Refolding intermediates of acid-unfolded mitochondrial aspartate aminotransferase bind to hsp70. *J. Biol. Chem.* **272**, 16852-16861.

Beckmann, R. P., Mizzen, L. E. and Welch, W. J. (1990). Interaction of Hsp 70 with newly synthesized proteins: implications for protein folding and assembly. *Science* **248**, 850-854.

Bedell, V. M., Yeo, S. Y., Park, K. W., Chung, J., Seth, P., Shivalingappa, V., Zhao, J., Obara, T., Sukhatme, V. P., Drummond, I. A. et al. (2005). roundabout4 is essential for angiogenesis in vivo. *Proc. Natl. Acad. Sci. USA* **102**, 6373-6378.

Chan, B., Sinha, S., Cho, D., Ramchandran, R. and Sukhatme, V. P. (2005). Critical roles of CD146 in zebrafish vascular development. *Dev. Dyn.* **232**, 232-244.

Durr, E., Yu, J., Krasinska, K. M., Carver, L. A., Yates, J. R., Testa, J. E., Oh, P. and Schnitzer, J. E. (2004). Direct proteomic mapping of the lung microvascular endothelial cell surface in vivo and in cell culture. *Nat. Biotechnol.* **22**, 985-992.

Fujio, Y. and Walsh, K. (1999). Akt mediates cytoprotection of endothelial cells by vascular endothelial growth factor in an anchorage-dependent manner. *J. Biol. Chem.* **274**, 16349-16354.

Galloway, J. L., Wingert, R. A., Thisse, C., Thisse, B. and Zon, L. I. (2005). Loss of gata1 but not gata2 converts erythropoiesis to myelopoiesis in zebrafish embryos. *Dev. Cell* **8**, 109-116.

Habeck, H., Odenthal, J., Walderich, B., Maischein, H. and Schulte-Merker, S. (2002). Analysis of a zebrafish VEGF receptor mutant reveals specific disruption of angiogenesis. *Curr. Biol.* **12**, 1405-1412.

Han, Z., Truong, Q. A., Park, S. and Breslow, J. L. (2003). Two Hsp70 family members expressed in atherosclerotic lesions. *Proc. Natl. Acad. Sci. USA* **100**, 1256-1261.

Hartl, F. U., Martin, J. and Neupert, W. (1992). Protein folding in the cell: the role of molecular chaperones Hsp70 and Hsp60. *Annu. Rev. Biophys. Biomol. Struct.* **21**, 293-322.

He, T. C., Zhou, S., da Costa, L. T., Yu, J., Kinzler, K. W. and Vogelstein, B. (1998). A simplified system for generating recombinant adenoviruses. *Proc. Natl. Acad. Sci. USA* **95**, 2509-2514.

Isogai, S., Lawson, N. D., Torrealday, S., Horiguchi, M. and Weinstein, B. M. (2003). Angiogenic network formation in the developing vertebrate trunk. *Development* **130**, 5281-5290.

Jowett, T. and Lettice, L. (1994). Whole-mount in situ hybridizations on zebrafish embryos using a mixture of digoxigenin- and fluorescein-labelled probes. *Trends Genet.* **10**, 73-74.

Kiang, J. G. and Tsokos, G. C. (1998). Heat shock protein 70 kDa: molecular biology, biochemistry, and physiology. *Pharmacol. Ther.* **80**, 183-201.

Kiang, J. G., Ding, X. Z. and McClain, D. E. (1998). Overexpression of HSP-70 attenuates increases in [Ca2+]i and protects human epidermoid A-431 cells after chemical hypoxia. *Toxicol. Appl. Pharmacol.* **149**, 185-194.

Kidd, K. R. and Weinstein, B. M. (2003). Fishing for novel angiogenic therapies. *Br. J. Pharmacol.* **140**, 585-594.

Kimmel, C. B., Ballard, W. W., Kimmel, S. R., Ullmann, B. and Schilling, T. F. (1995). Stages of embryonic development of the zebrafish. *Dev. Dyn.* **203**, 253-310.

Lawson, N. D. and Weinstein, B. M. (2002). In vivo imaging of embryonic vascular development using transgenic zebrafish. *Dev. Biol.* **248**, 307-318.

Marber, M. S., Mestril, R., Chi, S. H., Sayen, M. R., Yellon, D. M. and Dillmann, W. H. (1995). Overexpression of the rat inducible 70-kD heat stress protein in a transgenic mouse increases the resistance of the heart to ischemic injury. *J. Clin. Invest.* **95**, 1446-1456.

Merchan, J. R., Chan, B., Kale, S., Schnipper, L. E. and Sukhatme, V. P. (2003). In vitro and in vivo induction of antiangiogenic activity by plasminogen activators and captopril. *J. Natl. Cancer Inst.* **95**, 388-399.

Nasevicius, A. and Ekker, S. C. (2000). Effective targeted gene 'knockdown' in zebrafish. *Nat. Genet.* **26**, 216-220.

Plumier, J. C., Ross, B. M., Currie, R. W., Angelidis, C. E., Kazlaris, H., Kollias, G. and Pagoulatos, G. N. (1995). Transgenic mice expressing the human heat shock protein 70 have improved post-ischemic myocardial recovery. *J. Clin. Invest.* **95**, 1854-1860.

Polla, B. S., Healy, A. M., Wojno, W. C. and Krane, S. M. (1987). Hormone 1 alpha,25-dihydroxyvitamin D3 modulates heat shock response in monocytes. *Am. J. Physiol.* **252**, C640-C649.

Ribeiro, S. P., Villar, J., Downey, G. P., Edelson, J. D. and Slutsky, A. S. (1994). Sodium arsenite induces heat shock protein-72 kilodalton expression in the lungs and protects rats against sepsis. *Crit. Care Med.* **22**, 922-929.

Risau, W. and Flamme, I. (1995). Vasculogenesis. *Annu. Rev. Cell Dev. Biol.* **11**, 73-91.

Samali, A. and Cotter, T. G. (1996). Heat shock proteins increase resistance to apoptosis. *Exp. Cell Res.* **223**, 163-170.

Seth, P., Lin, Y., Hanai, J., Shivalingappa, V., Duyao, M. P. and Sukhatme, V. P. (2005). Magic roundabout, a tumor endothelial marker: expression and signaling. *Biochem. Biophys. Res. Commun.* **332**, 533-541.

Shiojima, I. and Walsh, K. (2002). Role of Akt signaling in vascular homeostasis and angiogenesis. *Circ. Res.* **90**, 1243-1250.

Snoeckx, L. H., Cornelussen, R. N., Van Nieuwenhoven, F. A., Reneman, R. S. and Van Der Vusse, G. J. (2001). Heat shock proteins and cardiovascular pathophysiology. *Physiol. Rev.* **81**, 1461-1497.

Steagall, R. J., Rusinol, A. E., Truong, Q. A. and Han, Z. (2006). HSPA12B is predominantly expressed in endothelial cells and required for angiogenesis. *Arterioscler. Thromb. Vasc. Biol.* (in press).

Sumanas, S., Jorniak, T. and Lin, S. (2005). Identification of novel vascular endothelial-specific genes by the microarray analysis of the zebrafish cloche mutants. *Blood* **106**, 534-541.

Takano, M., Arai, T., Mokuno, Y., Nishimura, H., Nimura, Y. and Yoshikai, Y. (1998). Dibutyryl cyclic adenosine monophosphate protects mice against tumor necrosis factor-alpha-induced hepatocyte apoptosis accompanied by increased heat shock protein 70 expression. *Cell Stress Chaperones* **3**, 109-117.

Thisse, B., Heyer, V., Lux, A., Alunni, V., Degrave, A., Seiliez, I., Kirchner, J., Parkhill, J. P. and Thisse, C. (2004). Spatial and temporal expression of the zebrafish genome by large-scale in situ hybridization screening. *Methods Cell Biol.* **77**, 505-519.

Weinstein, B. M., Stemple, D. L., Driever, W. and Fishman, M. C. (1995). Gridlock, a localized heritable vascular patterning defect in the zebrafish. *Nat. Med.* **1**, 1143-1147.

Westerfield, M. (2000). *The Zebrafish Book. A Guide for the Laboratory use of Zebrafish (Danio rerio).* Eugene, OR: University of Oregon Press.

Zhu, H., Traver, D., Davidson, A. J., Dibiase, A., Thisse, C., Thisse, B., Nimer, S. and Zon, L. I. (2005). Regulation of the lmo2 promoter during hematopoietic and vascular development in zebrafish. *Dev. Biol.* **281**, 256-269.